

Foto 12

**Pengukuran Data lapangan
(OS-05)**

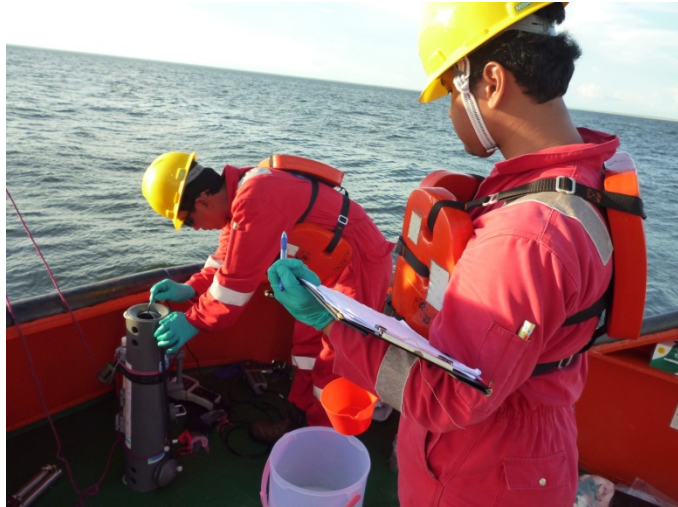


Foto 13

**Penyaringan sampel Air
Laut (OS-01)**



Foto 14

**Proses Penarikan sampel
Air laut (OS-11)**



Foto 15

**Pengukuran pH dan DO
(OS-02)**



Pengambilan Sampel Air Sumur

Foto 16

**Air Sumur Desa
Saengga (SGW01)**



Foto 17

**Air Sumur Desas
Saengga
(DGW01)**



Foto 18

**Air Sumur Desa
Saengga (DGW02)**



Pengukuran Arus

Foto 19

**Pembacaan Arus
(OS-03)**



Foto 20

**Pengukuran Arus
(NS-09)**



Foto 21

Pengukuran Arus (OS-05)



Foto 22

Penurunan Current Meter (OS-05)

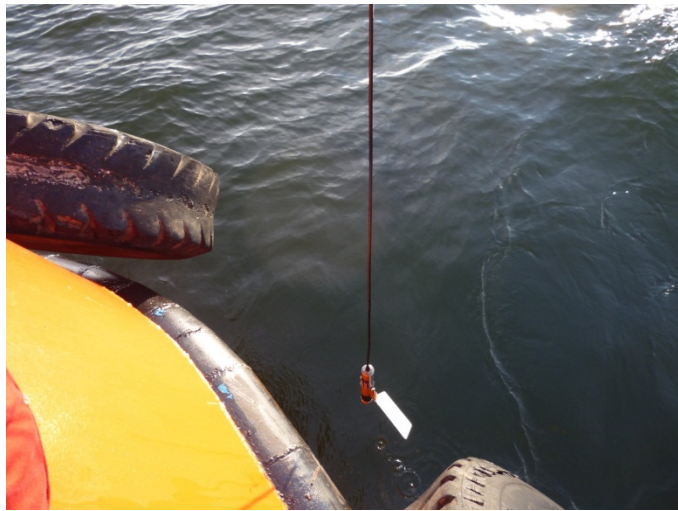


Foto 23

Penurunan Current Meter (OS-01)



Foto 24

Pengukuran pH dan DO
(OS-02)



Benthos

Foto 25

Hasil ayakan sedimen
(NS-04)



Foto 26

Hasil ayakan Sedimen
(NS-07)



Foto 27
Proses pengayakan
(OS-02)



Foto 28
Hasil ayakan
Sedimen (OS-02)

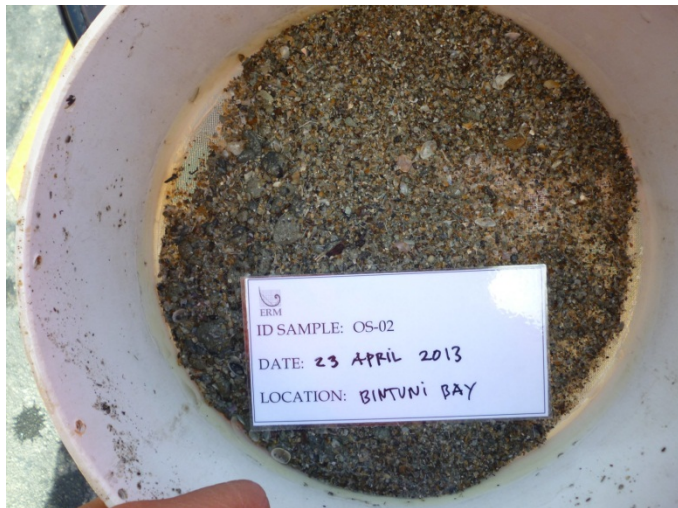


Foto 29
Proses Pengayakan
Sedimen
(OS-04)



Foto 30
Hasil ayakan Sedimen
(OS-04)



Foto 31
Hasil ayakan Sedimen
(OS-05)

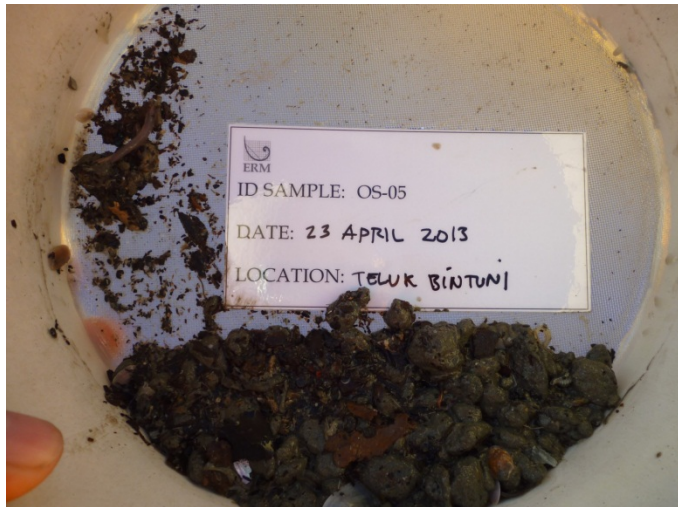
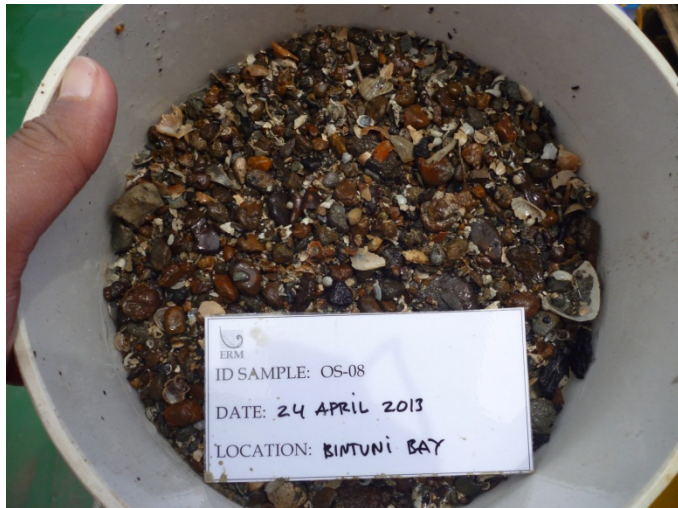


Foto 32
Hasil ayakan sedimen
(OS-08)



Penurunan CTD

Foto 33

Penurunan CTD (OS-03)



Foto 34

**Penurunan CTD
(OS-14)**



Foto 35

**Persiapan penurunan
CTD (NS-05)**



Foto 36

**Penurunan CTD
(NS-07)**



Foto 37

**Penurunan CTD
(NS-08)**



Foto 38

**Penurunan CTD
(OS-02)**



Pengambilan Sampel Plankton

Foto 39

**Sampling Plankton
(OS-03)**



Foto 40

**Samplin Plankton
(NS-05)**



Foto 41

**Sampling Plankton
(SW-03)**



Foto 42
Pengambilan Plankton
(NS-08)



Foto 43
Samplng Plankton
(OS-02)



Pengambilan Sampel Sedimen

Foto 44
Sampel Sedimen
(OS-03)



Foto 45

**Sampel Sedimen
(OS-06)**



Foto 46

**Sampel Sedimen
(SW-03)**



Foto 47

**Pengambilan Sampel
Sedimen
(NS-06)**



Foto 48
Sampel Sedimen (OS-14)



Foto 49
Pengambilan sampel sedimen (NS-07)



Foto 50
Sampel Sedimen (NS-07)



Foto 51

Pengambilan sampel sedimen (NS-08)



Foto 52

Pengambilan Sampel Sedimen (NS-08)



Foto 53

Pengambilan Sampel Sedimen (NS-09)



Foto 54

**Penurunan Grap
Sampler (OS-02)**



Foto 55

**Pengambilan
sampel sedimen
(OS-02)**

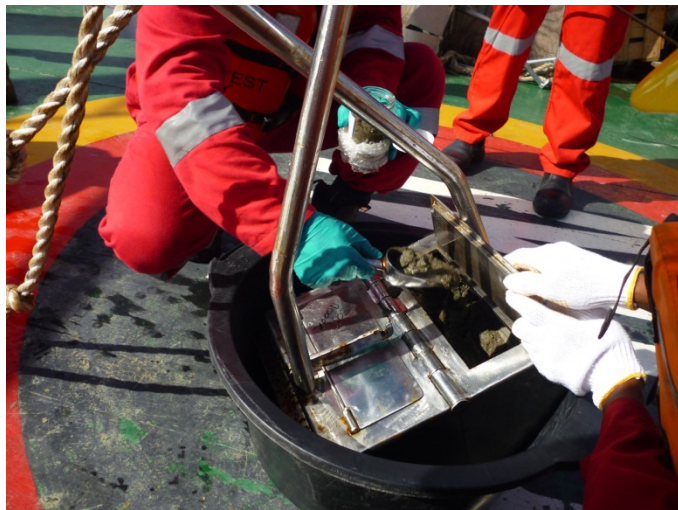


Foto 56

**Sampel Sedimen
(OS-02)**

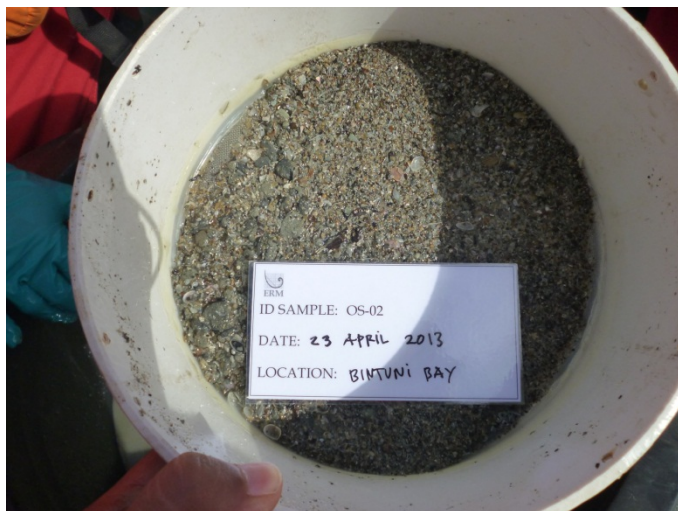


Foto 57

**Penurunan Grap Sampler
(OS-04)**



Foto 58

**Penarikan Grap Sampler
(OS-04)**



Foto 59

Sampel Sedimen (OS-04)



Foto 60

**Sampel Sedimen
(OS-05)**

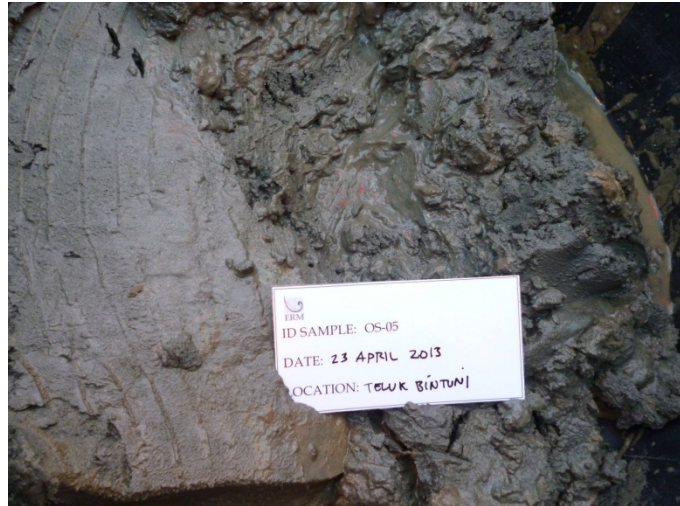


Foto 61

**Persiapan Penurunan
Grap Sampler
(OS-01)**



Foto 62

**Proses Penurunan
Grap Sampler
(OS-01)**



Foto 63
Proses Penarikan Grab
(OS-08)



Pengambilan Sampel Udara Ambien

Foto 64
Udara ambien di
Helipad (AQ-01)

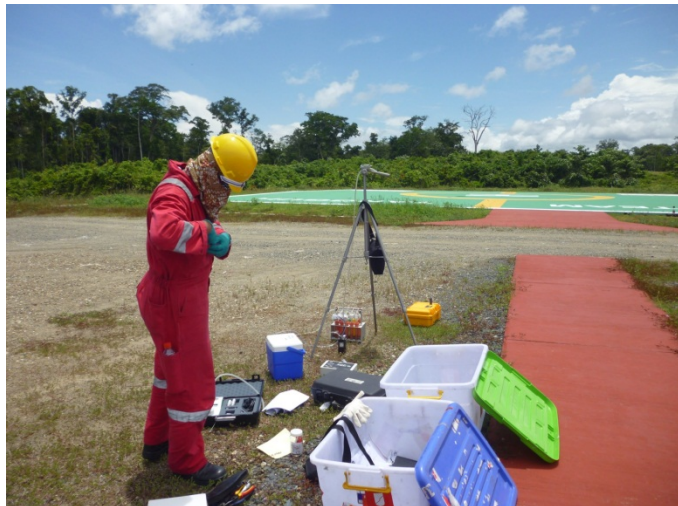


Foto 65
Udara ambien di
belakang Mess
(AQ-06)



Foto 66

**Udara ambien di Arguni
(AQ-08)**



Foto 67

**Udara ambien di Kapal
(AQ-10)**



Lampiran IV

Hasil Permodelan

Lampiran IV. 1

Drilling Cutting and Mud Dispersion Simulation



Drilling Cutting and Mud Dispersion Simulation



Final Report



January 2012

Drilling Cutting and Mud Dispersion Study

TABLE OF CONTENTS

Contents

Contents.....	i
Chapter 1 Introduction.....	1-1
1.1 Background.....	1-1
1.2 Objectives.....	1-1
1.3 Scope of Work.....	1-1
1.4 This Report.....	1-2
Chapter 2 Description of Study Area.....	2-1
Chapter 3 Model Description.....	3-1
3.1 Background.....	3-1
3.2 Governing Equations.....	3-2
Chapter 4 Model Setup and Validation.....	4-1
4.1 Boundary Fitted Grid System of Large Scale Domain.....	4-1
4.2 Bathymetric of Large Scale Domain.....	4-1
4.3 Open Boundary of Large Scale Domain.....	4-1
4.4 Small Scale Domain.....	4-2
4.5 Simulation Scenario.....	4-2
4.6 Validation.....	4-4
Chapter 5 Model Results.....	5-1
5.1 Ofweri-2 Well.....	5-2
5.2 Roabiba-2 Well.....	5-8
5.3 Vorwata-12 Well.....	5-15
5.4 Teteruga-2 Well.....	5-21
Chapter 6 Conclusions.....	6-1

Contents

References

- Appendix A Simulation Result of Cutting at Ofaweri-2 Well
- Appendix B Simulation Result of Cutting at Roabiba-2 Well
- Appendix C Simulation Result of Cutting at Vorwata-12 Well
- Appendix D Simulation Result of Cutting at Teteruga-2 Well
- Appendix E Simulation Result of Arsenic in Cutting at Ofaweri-2 Well
- Appendix F Simulation Result of Arsenic in Cutting at Roabiba-2 Well
- Appendix G Simulation Result of Arsenic in Cutting at Vorwata-12 Well
- Appendix H Simulation Result of Arsenic in Cutting at Teteruga-2 Well
- Appendix I Simulation Result of Mud at Dumping Location 1 (East)
- Appendix J Simulation Result of Mud at Dumping Location 2 (West)

Drilling Cutting and Mud Dispersion Study

Chapter **1**

INTRODUCTION

Introduction

1.1 Background

BP and Tangguh-LNG plans to initiate Tangguh Exploration and Appraisal Project at Bintuni Bay, Babo district, Bintuni Bay Regency, Papua Barat. As part of the Project activities, it intends to discharge the drilling cutting and mud into the sea. LAPI-ITB was commissioned to conduct dispersion modeling using MuQual3D software to assess the potential impacts from the discharge into the environmental and to obtain the necessary discharge permit from Ministry of Environment.

1.2 Objectives

The basic objectives of the study are to conduct long term simulation dispersion of physical and chemical properties of Drilling Cuttings and Mud using three dimensional hydrodynamics and water quality model (MuQual3D).

1.3 Scope of Work

The scope of the work includes:

- ¾ To report summarizing the modeling methodology used.
- ¾ To run Model.
- ¾ To present and socialize the results of modeling to Tangguh LNG, the Ministry of Environment, and BP Migas.
- ¾ To submit the results of study in Final Report.

1.4 This Report

This report provides a detail description of the modeling work. **Chapter 2** presents the description of study area. **Chapter 3** describes the state of the art of the boundary fitted

three-dimensional model. **Chapter 4** describes model setup. **Chapter 5** shows the modeling results. **Chapter 6** presents the conclusions of the study.

Drilling Cutting and Mud Dispersion Study

Chapter **2**

DESCRIPTION OF STUDY AREA

Description of Study Area

The study area is in Berau/Bituni Bay, Papua Province, Indonesia (**Figure 2.1**). Bituni Bay is approximately 160km long, and about 50km wide at the opening. The Environmental Sensitivity Index Mapping of the study area can be seen in Figure 2.2.

As reported in Berau Bay Seabed Morphology Study (Document 9000-SDY-PL-0010), there is little wave action in the bay. A significant wave height of 1m has a non-exceedance probability of 99.7%, and the 100 year return period condition is estimated as a wave height of 3.4m and a peak period of 7s. In 30m water depth this gives an orbital velocity of 0.2m/s. Tidal current measurements indicate peak tidal current magnitudes of 1.5 to 2m/s. Therefore the bottom orbital velocities due to waves and the induced bed shear stresses will have a negligible effect on the seabed dynamics compared with those from the usual tidal currents.

Berau and Bintuni bays comprise a large expanse of shallow water, exhibiting some estuarine characteristics, including substantial variation in salinity and high concentrations of suspended particulates, particularly during the wet season. Water temperature ranges from 24°C to 30°C throughout the bays, and salinity generally ranges from 26 to 32 psu. Suspended particulate concentrations commonly reach 200–300 milligram per liter (mg/L) close to the shore, with even higher concentrations near the seabed. Suspended sediment levels decline rapidly away from the shore as a result of flocculation and deposition. Tides are semidiurnal with an astronomical range of approximately 4 m. Currents are tidally driven, with a maximum speed of 1.9 meter per second (m/sec) measured in the study area.

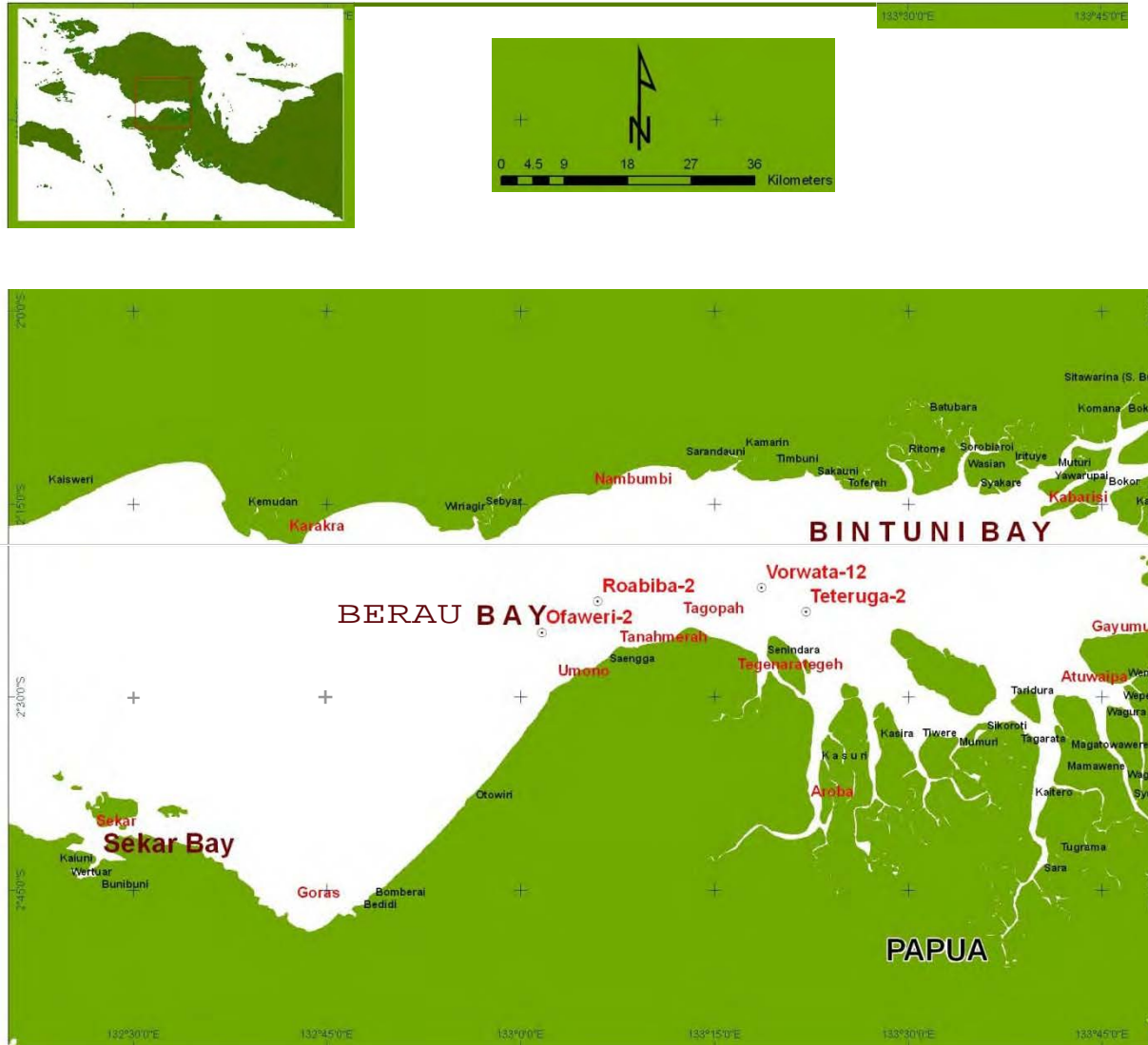


Figure 2.1 Area of Study Berau/Bintuni Bay, Papua Province, Indonesia

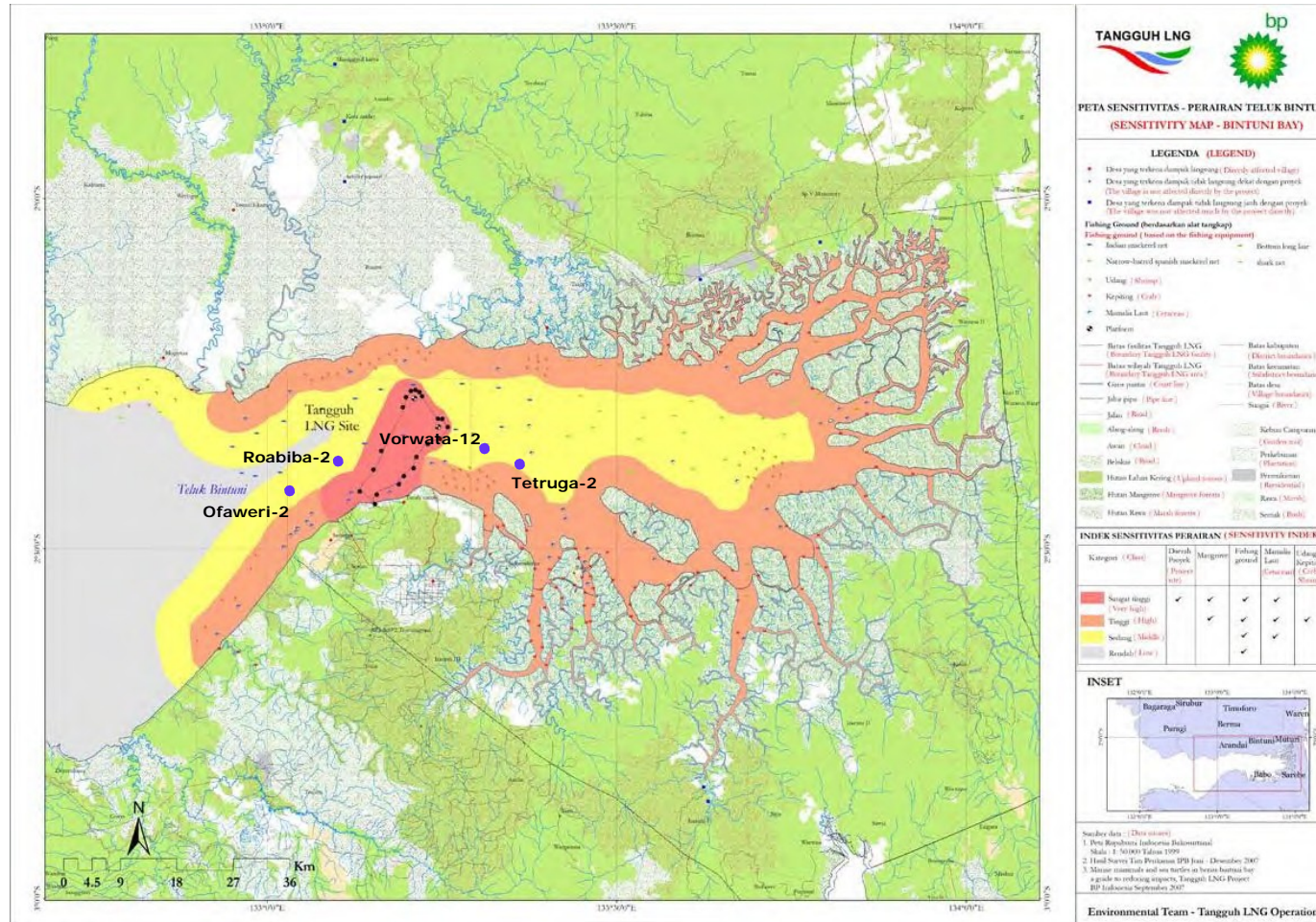


Figure 2.2 Environmental Sensitivity Index of Berau/Bintuni Bay

Drilling Cutting and Mud Dispersion Study

Chapter **3**

MODEL DESCRIPTION

Model Description

3.1 Background

Development and application of hydrodynamic models to predict circulation in estuarine, coastal and shelf water has been extremely active over the past two decades (**Spaulding *et al.*** 1990) with the majority of studies employing finite difference techniques on a rectangular grid. While this has proven useful in various applications, it becomes expensive and impractical when the study area is geometrically and bathymetrically complex. Excessive numerical truncation error may arise from too few grids representing too complex a geometry, while computational cost prevents the use of more refined grid resolution. Such difficulties have motivated the introduction of curvilinear coordinate.

Anticipating the use of hydrodynamic model with substantial variation in latitude, **Spaulding** (1984) developed a boundary fitted spherical coordinate model and solved vertically averaged equations of motion using **Leendertsee's** (1967) multi-operational method in curvilinear coordinates. **Muin** (1993) further improved the model by transforming both the dependent variables (the velocity components) as well as the independent variables (coordinate geometry) into curvilinear coordinates and introducing a three dimensional solution using a split technique in which the governing equations are divided into an exterior (vertically averaged) and interior modes (vertical structure).

The study will utilize MuDrillCutting3D as module of software MuQual3D, the state-of-the-art Non-Orthogonal Boundary Fitted Hydrodynamics and Water Quality Model for this application. The Boundary Fitted Hydrodynamics Model uses a variable grid which enables great flexibility in model grid design. The variable grid design has the flexibility to allow area of interest in the model domain to be gridded at higher resolution as required with coarser grid elsewhere. Further, the non-orthogonal boundary fitted hydrodynamics model provides accurate hydrodynamic prediction than orthogonal techniques. MuQual3D predicts the dynamic of conservative and non-conservative pollutant transport and dispersion of the discharged material.

MuQual3D is integrated model, in which consists of following model:

- ¾ 3D Water Quality Model,
- ¾ 3D Drilling Cutting and Mud Model (MuDrillCutting3D)
- ¾ 3D Ocean Hydrodynamics Model (MuHydro3D),
- ¾ Embedded Arc View Geographic Information System (GIS).

3.2 Governing Equations

The mathematical basis for the model begins with continuity and momentum equations. Both equations were developed with the underlying assumption that the flow is incompressible, variation of water mass density negligible except when multiplied with the earth's gravity (Boussinesq approximation), vertical acceleration negligible as compared to gravitational acceleration (hydrostatic approximation).

As boundary condition along shoreline, the beach is assumed as impermeable surface where there is no fluid particle velocity normal to it. Time varying water surface elevation commands the boundary condition at the ocean side. Influxes from rivers may be included by specifying their discharge. Two options are available to specify shear stresses at the bottom: (1) quadratic stress law or (2) Manning coefficient. At the free surface, the wind stress is calculated using quadratic approximation.

In order to perform computation in curvilinear system, where the mesh is made up of square grids, both dependent and independent variables in the above three equations are transformed into a curvilinear coordinate system. The vertically averaged equations of mass conservation (continuity) and motion in the (ξ, η) curvilinear system written in terms of contra variant velocity components are as follows.

Continuity

$$Jr \cos \theta \frac{\partial \xi}{\partial t} + \frac{\partial}{\partial \zeta} (\cos \theta J u^c D) + \frac{\partial}{\partial \eta} (\cos \theta J v^c D) + Jr \cos \theta \frac{\partial (\omega D)}{\partial \sigma} = \frac{Q_R}{r} \quad (1)$$

Momentum Equation

• ξ -direction

$$\begin{aligned}
 \frac{\partial u^c D}{\partial t} &= -\frac{\theta_\eta \theta_\eta + \cos^2 \theta \varphi_\eta \varphi_\eta}{J^2 \rho_0 r \cos^2 \theta} \frac{Dg}{2} \left[\{\lambda + (\rho_s - 2\rho)(1 - \sigma)\} \frac{\partial D}{\partial \zeta} + (4\rho - 2\rho_s) \frac{\partial \zeta}{\partial \zeta} + D \frac{\partial \lambda}{\partial \zeta} \right] \\
 &+ \frac{\theta_\zeta \theta_\eta + \cos^2 \theta \varphi_\zeta \varphi_\eta}{J^2 \rho_0 r \cos^2 \theta} \frac{Dg}{2} \left[\{\lambda + (\rho_s - 2\rho)(1 - \sigma)\} \frac{\partial D}{\partial \eta} + (4\rho - 2\rho_s) \frac{\partial \zeta}{\partial \eta} + D \frac{\partial \lambda}{\partial \eta} \right] \\
 &- \frac{\theta_\eta}{J^2 r \cos^2 \theta} \left[\frac{\partial}{\partial \zeta} (\varphi_\zeta \cos^2 \theta Ju^c u^c D + \varphi_\eta \cos^2 \theta Ju^c v^c D) + \frac{\partial}{\partial \eta} (\varphi_\zeta \cos^2 \theta Ju^c v^c D + \varphi_\eta \cos^2 \theta Jv^c v^c D) \right] \\
 &+ \frac{\varphi_\eta}{J^2 r \cos^2 \theta} \left[\frac{\partial}{\partial \zeta} (\theta_\zeta \cos^2 \theta Ju^c u^c D + \theta_\eta \cos^2 \theta Ju^c v^c D) + \frac{\partial}{\partial \eta} (\theta_\zeta \cos^2 \theta Ju^c v^c D + \theta_\eta \cos^2 \theta Jv^c v^c D) \right] \\
 &- \frac{\partial}{\partial \sigma} (\omega u^c D) + \frac{fD}{J \cos \theta} \left[(\theta_\zeta \theta_\eta + \cos^2 \theta \varphi_\zeta \varphi_\eta) u_c + (\theta_\eta \theta_\eta + \cos^2 \theta \varphi_\eta \varphi_\eta) v^c \right] + \frac{4}{D} \frac{\partial}{\partial \sigma} \left(A_v \frac{\partial u^c}{\partial \sigma} \right)
 \end{aligned} \tag{2}$$

• η -direction

$$\begin{aligned}
 \frac{\partial v^c D}{\partial t} &= \frac{\theta_\eta \theta_\xi + \cos^2 \theta \varphi_\eta \varphi_\xi}{J^2 \rho_0 r \cos^2 \theta} \frac{Dg}{2} \left[\{\lambda + (\rho_s - 2\rho)(1 - \sigma)\} \frac{\partial D}{\partial \xi} + (4\rho - 2\rho_s) \frac{\partial \zeta}{\partial \xi} + D \frac{\partial \lambda}{\partial \xi} \right] \\
 &- \frac{\theta_\xi \theta_\xi + \cos^2 \theta \varphi_\xi \varphi_\xi}{J^2 \rho_0 r \cos^2 \theta} \frac{Dg}{2} \left[\{\lambda + (\rho_s - 2\rho)(1 - \sigma)\} \frac{\partial D}{\partial \eta} + (4\rho - 2\rho_s) \frac{\partial \zeta}{\partial \eta} + D \frac{\partial \lambda}{\partial \eta} \right] \\
 &+ \frac{\theta_\xi}{J^2 r \cos^2 \theta} \left[\frac{\partial}{\partial \xi} (\varphi_\xi \cos^2 \theta Ju^c u^c D + \varphi_\eta \cos^2 \theta Ju^c v^c D) + \frac{\partial}{\partial \eta} (\varphi_\xi \cos^2 \theta Ju^c v^c D + \varphi_\eta \cos^2 \theta Jv^c v^c D) \right] \\
 &- \frac{\varphi_\xi}{J^2 r \cos^2 \theta} \left[\frac{\partial}{\partial \xi} (\theta_\xi \cos^2 \theta Ju^c u^c D + \theta_\eta \cos^2 \theta Ju^c v^c D) + \frac{\partial}{\partial \eta} (\theta_\xi \cos^2 \theta Ju^c v^c D + \theta_\eta \cos^2 \theta Jv^c v^c D) \right] \\
 &- \frac{\partial}{\partial \sigma} (\omega v^c D) - \frac{fD}{J \cos \theta} \left[(\theta_\xi \theta_\xi + \cos^2 \theta \varphi_\xi \varphi_\xi) u_c + (\theta_\xi \theta_\eta + \cos^2 \theta \varphi_\xi \varphi_\eta) v^c \right] + \frac{4}{D} \frac{\partial}{\partial \sigma} \left(A_v \frac{\partial v^c}{\partial \sigma} \right)
 \end{aligned} \tag{3}$$

In addition, the equation for conservation of substance and the equation of state are also required to take into account sediment, salinity, and temperature. These equations are as follows:

Conservation of Substance

$$\begin{aligned} \frac{\partial q}{\partial t} + \frac{u^c}{r} \frac{\partial q}{\partial \xi} + \frac{v^c}{r} \frac{\partial q}{\partial \eta} + \omega \frac{\partial q}{\partial \sigma} = \frac{4}{D^2} \frac{\partial}{\partial \sigma} \left(D_v \frac{\partial q}{\partial \sigma} \right) \\ + \frac{D_h}{r^2 J^2} \left[\left(\frac{\theta_\eta \theta_\eta}{\cos^2 \theta} + \varphi_\eta \varphi_\eta \right) \frac{\partial^2 q}{\partial \xi^2} - 2 \left(\frac{\theta_\xi \theta_\eta}{\cos^2 \theta} + \varphi_\xi \varphi_\eta \right) \frac{\partial^2 q}{\partial \xi \partial \eta} + \left(\frac{\theta_\xi \theta_\xi}{\cos^2 \theta} + \varphi_\xi \varphi_\xi \right) \frac{\partial^2 q}{\partial \eta^2} \right] - Kq \end{aligned} \quad (4)$$

Equation of State

$$\rho = \text{function of } (S, \Theta) \quad (5)$$

Where:

- ξ, η = curvilinear coordinates
- φ, θ = longitude, latitude
- t = time
- f = Coriolis parameter
- g = gravitational acceleration
- ρ' = vertical density difference ($\rho = \bar{\rho} + \rho'$)
- $\bar{\rho}$ = vertically-averaged mass density of water
- ρ_o = basin-averaged mass density of water
- ρ_s = water density at the surface
- ω = vertical velocity in σ -coordinate
- σ = sigma stretching coordinate
- ζ = water surface deviation from mean level
- h = water depth
- D = $h + \zeta$
- A_v = vertical eddy viscosity
- D_v = vertical eddy diffusivity
- D_h = horizontal eddy diffusivity
- r = radius

- R = earth's radius
 S = salinity (ppt)
 θ = temperature in centigrade
 q = concentration of substance
 Ω^n = concentration of n-th class of suspended sediment material
 u^c, v^c = contravariant velocities in the (ξ, η) directions, respectively
 Q_r = River flow or water exchange discharge from or into mangrove
 J = Jacobian = $\varphi_\xi \theta_\eta - \varphi_\eta \theta_\xi$

The relationship between the contravariant velocities (u^c, v^c) and velocities in spherical coordinates (u, v) is given by

$$u = \cos\theta \varphi_\xi u^c + \sin\theta \varphi_\eta v^c \quad (7)$$

$$v = \theta_\xi u^c + \theta_\eta v^c \quad (8)$$

The above governing equations were solved numerically using a semi-implicit technique where water surface elevation in the long wave equation was solved implicitly and the other variables explicitly. By adopting this combination, the time- step size in the numerical solution was not constrained by the shallow water wave celerity, hence rapid computer execution. Detailed description of the hydrodynamics model can be found in **Muin (1993)**.

Drilling Cutting and Mud Dispersion Study

Chapter **4**

MODEL SETUP AND VALIDATION

Model Setup and Validation

The simulations are performed in large-scale and small-scale nested computational domain. The large-scale model covers from Bintuni Bay and Berau Bay. Along open boundary of large scale domain, sea surface elevation was specified with time series of water elevation that is generated from tidal components. The amplitude and phase of each tidal component are obtained from Global Tidal Model. The salinity in open boundary is assumed constant.

4.1 Boundary Fitted Grid System of Large Scale Domain

For modeling purposes, the Bintuni and Berau Bay need to be discretised into computational grids. The main water body was represented by non-orthogonal boundary fitted grid system. The model employed 20 levels sigma-stretching coordinate to resolve vertical structure of current and salinity concentration in water column.

The computational grid is shown in **Figure 4.1**. The main water bodies are represented by 2530 boundary fitted water grid. The grid sizes range from 20 meters to 300 meters.

4.2 Bathymetry of Large Scale Domain

The bathymetric data in study area was obtained from the Hidral Map and measurement by Tangguh Project. **Figure 4.2** shows the grid bathymetry adopted by the model. The water depths along the coast are typically 2 to 13 meter. The middle of Bay ranges from 15 meters to 50 meters.

4.3 Open Boundary of Large Scale Domain

The Open Boundary is located at the mouth of Bintuni Bay (Arafura Sea). Open boundaries should ideally be placed further away from the area of interest to minimize the effect of boundary conditions on the model.

Nine major tidal components (M2, S2, N2, O1, K1, M4, M6, P1, and Q1) were used to generate tidal elevation along open boundary. The water elevation for each grid was further analyzed to obtain tidal component and presented in **Tables 4.1**.

Table 4.1 Tidal Amplitude and Phase

Open Boundary

Tidal Component	Amplitude (meter)	Phase (degree)
M2	0.4717	185.9
N2	0.1119	179.4
S2	0.1926	240.7
K1	0.2249	201.9
O1	0.1666	183.0
M4	0.0015	158.5
M6	0.0009	58.4
P1	0.0744	200.6
Q1	0.0323	173.6

4.4 Small Scale Domain

The small-scale nested model is performed using 200x200, 50 meters square-grid system in the near region of outlet. The dynamics of water currents are obtained from output of large-scale simulation.

4.5 Simulation Scenario

Location of Drilling Activity and Dumping of Mud is shown in **Figure 4.5**. Data of wells for drilling activities presented in **Table4.2**. The dispersion simulation in was conducted under 4 Stages Drilling Cutting Scenario as follows:

Table 4.2 Data of Well

Well Section	Drilling Time (days)	Discharge Volume (MT)	Discharge Rate (MT/hour)	Rock Type	Remarks
24□	1.3	686	21.9	80-90□ shale, 10□ sandstone	Seawater
17 □□	7	1166	6.9	80-90□ shale, 10□ sandstone	Water □ase mud (□entonite □ase)
12 □□	1.5	207	5.3	Limestone	Drilling with sea water, total losses, no return, no cuttings
8 □□	15.8	463	1.2	50□ shale, 50□ sandstone	Water □ase mud
Well Cleanup	1	420	17.5	Water □ased mud	This is end well clean up for each well □efore rig move

The data of discharge are provided by BP Tangguh LNG which is based on the drilling data for one complete well in Vorwata field. Estimated mud is presented in **Table 4.3**. The related heavy metal properties for cutting sediment data are based on sampling bed sediment near area (**Table 4.4**).

Table 4.3 Estimated Mud Discharge

Discharge	Mud Volume (bbl)	Mud Weight (lb/gal)	Mud Solids Fraction	Volume of Solids in Mud (bbl)	Weight of Dry Solids in Mud (mt)
Batch Completion	2500	9.0	0.03393	84.8	35.1
Cementing 13 5/8 inch casing (per well)	500	9.0	0.03393	17.0	7.0

Table 4.4 Arsenic properties on Sediment

	Unit	Detection Limit	Sediment Standard (CCME, 1999)		AVERAGE SAMPLE RESULT			
			ISQGs	PEL	V-12	Roa-2	Ofa-2	Te-2
Arsenic	mg/dry Kg	0.2	7.24	41.6	60.6	161.3	28.3	7.9

4.6 Validation

The success of any model application depends on the credibility of the model predictions. This credibility is gained by careful comparison of model predictions with observations.

The purpose of calibration is to select model coefficient to best match observation data. The primary calibrations data for this software are the observed water elevation and current from oceanographic survey by Calmarine (1999). The agreements between model and field data are excellent.

The bottom frictions in the main water body, turbulence model parameter were tuned to match the water elevation and current measurement data. The comparison between the predicted and observed water elevation and Current are presented in **Figure 4.3** and **Figure 4.4**.

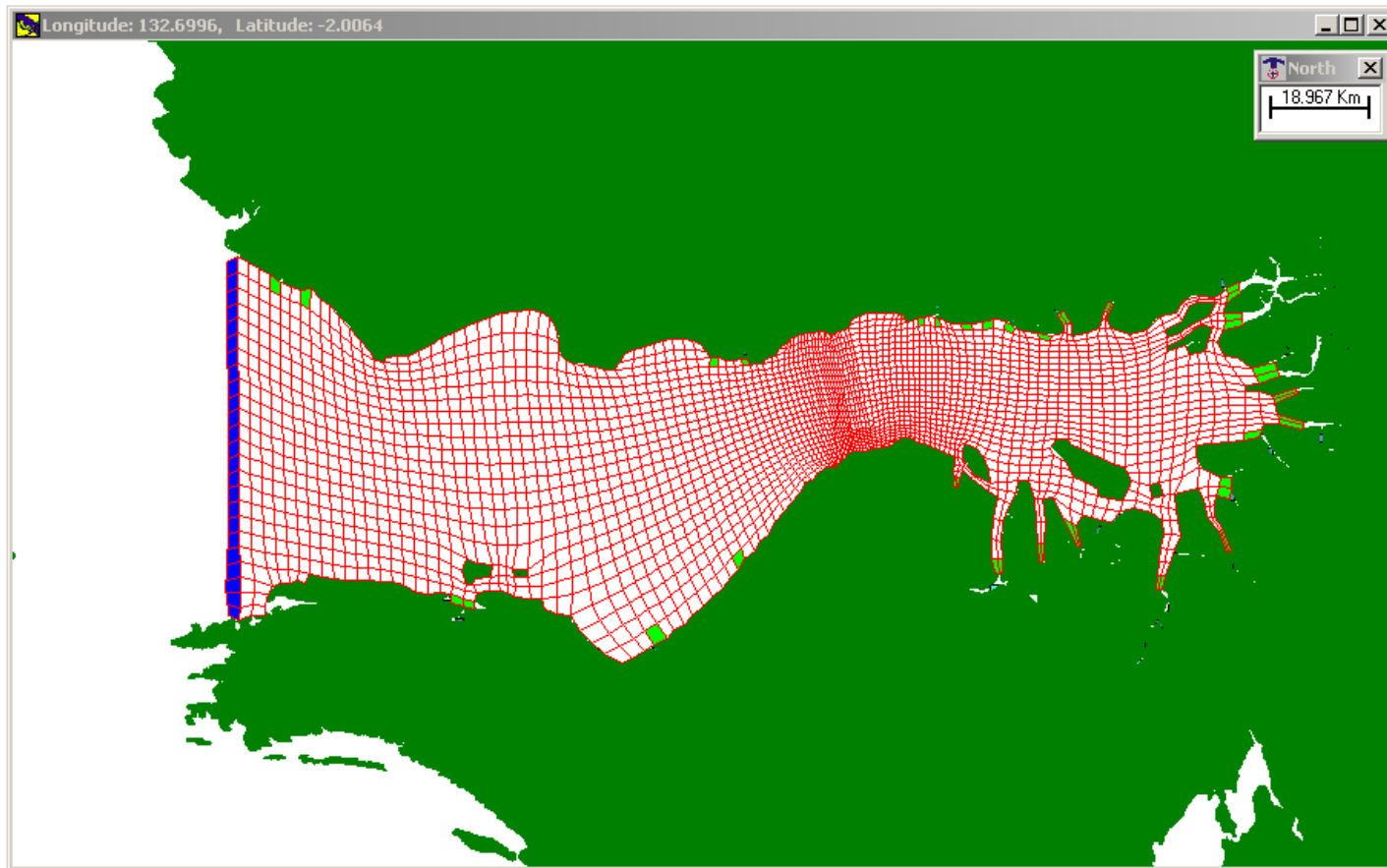


Figure 4.1 Non-Orthogonal Boundary Fitted Grid in Large-Scale Model

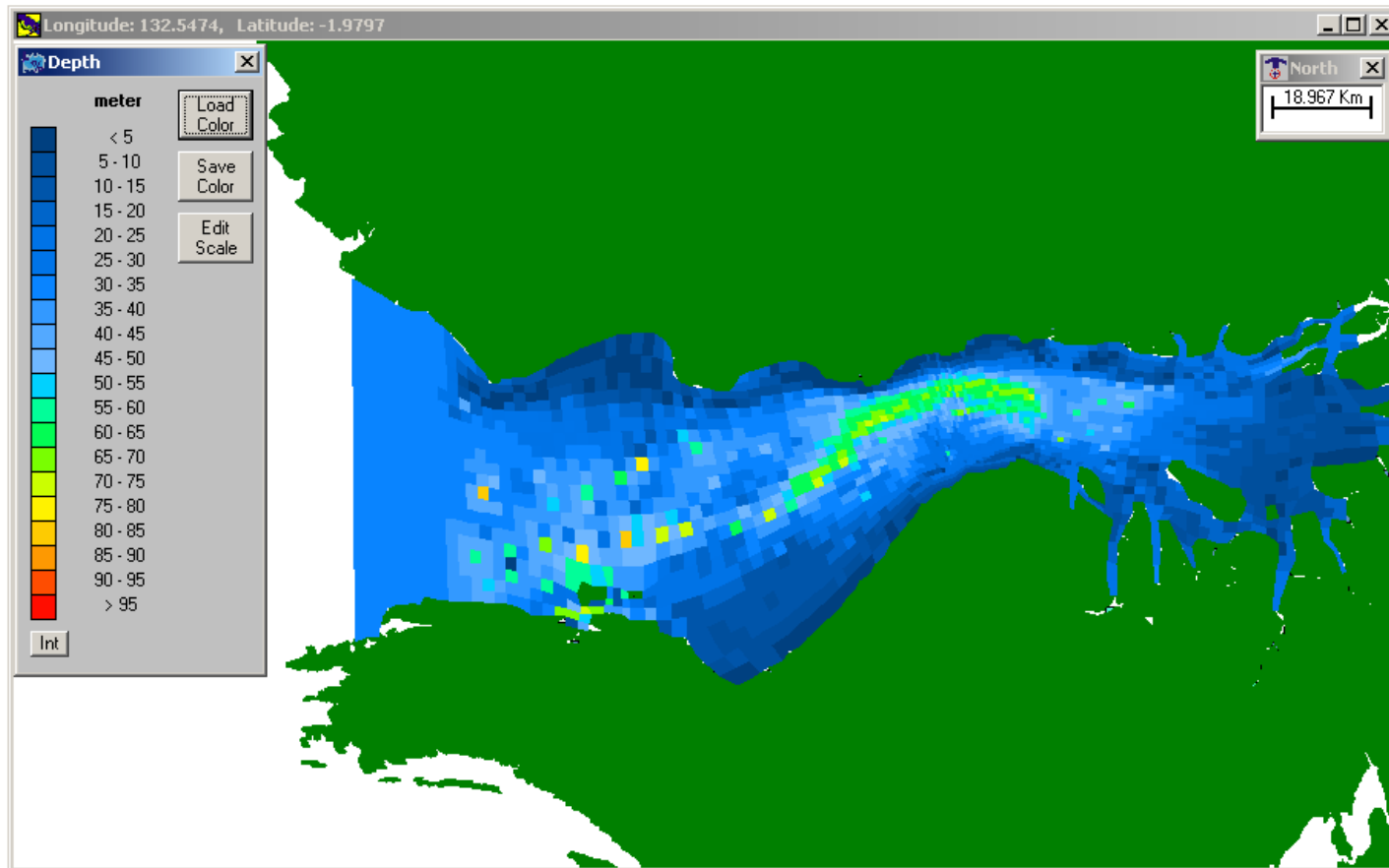


Figure 4.2 Bathymetric in Large-Scale Model